Temperature-dependent optical properties of hexagonal and cubic $Mg_xZn_{1-x}O$ thin-film alloys

2004 J. Phys.: Condens. Matter 16 2973

(http://iopscience.iop.org/0953-8984/16/17/024)

INSTITUTE OF PHYSICS PUBLISHING JOURNAL OF PHYSICS: CONDENSED MATTER

J. Phys.: Condens. Matter **16** (2004) 2973–2980 PII: S0953-8984(04)66882-2

Temperature-dependent optical properties of hexagonal and cubic $Mg_xZn_{1-x}O$ thin-film alloys

N B Chen[1], H Z Wu[1,3], D J Qiu[1], T N Xu[1], J Chen[2] and W Z Shen[2]

[1] Department of Physics, Zhejiang University, Hangzhou 310028, People's Republic of China
[2] Department of Physics, Laboratory of Condensed Matter Spectroscopy and Opto-Electronic Physics, Shanghai Jiao Tong University, Shanghai 200030, People's Republic of China
[3] State Key Laboratory of Functional Materials for Informatics, Shanghai Institute of Microsystem and Information Technology, CAS, Shanghai 200050, People's Republic of China

E-mail: hzwu@zju.edu.cn

Received 31 July 2003
Published 16 April 2004
Online at stacks.iop.org/JPhysCM/16/2973
DOI: 10.1088/0953-8984/16/17/024

Abstract

Both hexagonal and cubic $Mg_xZn_{1-x}O$ ($0 \leqslant x \leqslant 0.6$) films were grown on c-plane (0001) sapphire substrate at low temperature. X-ray diffraction measurements show that the cubic $Mg_xZn_{1-x}O$ films grow along the [111] direction while the hexagonal ZnO films grow along [0001]. The temperature-dependent optical properties of $Mg_xZn_{1-x}O$ films were measured by ultraviolet optical transmission with temperature variation from 10 to 300 K and analysed by theoretically fitting the optical absorption spectra. For $Mg_xZn_{1-x}O$ with $0 < x \leqslant 0.51$, only stable hexagonal phase was observed and the optical absorption edge red shifts with temperature increase monotonically. For $Mg_xZn_{1-x}O$ with $x \geqslant 0.55$, the crystal structure is cubic at 300 K. However, as measurement temperature decreases from 300 to 10 K an abnormality of the optical absorption is observed, which is attributed to the possible phase transition from cubic to hexagonal structure. The underlying physical mechanism for the crystal phase transition is attributed to the interaction of stress with stacking faults in the cubic $Mg_xZn_{1-x}O$.

1. Introduction

ZnO is a wide-bandgap II–VI semiconductor with large exciton binding energy (∼60 meV). It has attracted considerable attention due to the possibility of fabricating reliable high-efficiency photonic devices based on ZnO, such as solar cells, transparent conductors for displays, light emitters, sensors, modulators and UV detectors [1]. To fabricate ZnO heterostructure devices, ternary $Mg_xZn_{1-x}O$ alloy has been synthesized recently because $Mg_xZn_{1-x}O$ has even wider bandgap than that of ZnO [2–4]. As Mg concentration in $Mg_xZn_{1-x}O$ increases from zero to unity, the crystalline structure changes from hexagonal to cubic phase and the bandgap enlarges

from 3.3 to 7.7 eV. On sapphire substrates, Ohtomo *et al* [2] have grown hexagonal $Mg_xZn_{1-x}O$ films ($0 \leqslant x \leqslant 0.33$), and Choopun *et al* [3] have reported metastable cubic-phase $Mg_xZn_{1-x}O$ films ($0.5 \leqslant x \leqslant 1$) using the pulsed laser deposition (PLD) method. On Si substrates, Qiu *et al* [4] have successfully fabricated cubic $Mg_xZn_{1-x}O$ films at low growth temperature. But to the authors' knowledge, few reports on temperature-dependent optical and electronic characterizations for either hexagonal or cubic $Mg_xZn_{1-x}O$ films have been published. It is still uncertain what is the exact Mg composition at which $Mg_xZn_{1-x}O$ crystal changes from hexagonal to cubic phase. For example, Choopun *et al* found that if the Mg concentration in $Mg_xZn_{1-x}O$ was up to ∼36 at.% the ternary alloy had hexagonal structure, within the Mg composition range of 36–43 at.% it was a mixed region of both hexagonal and cubic phases and when the Mg concentration was higher than 43 at.% it had metastable cubic phase. However, according to the results reported by Yi *et al* [5], hexagonal-phase $Mg_xZn_{1-x}O$ film with Mg concentration equal to 49 at.% has been obtained. Furthermore, the studies of temperature-dependent optical properties of both hexagonal and cubic $Mg_xZn_{1-x}O$ films have not been reported. In this paper, the transmittance spectra measurements with temperature varied from 10 to 300 K for both hexagonal $Mg_xZn_{1-x}O$ ($x \leqslant 0.51$) and cubic $Mg_xZn_{1-x}O$ ($x \geqslant 0.55$) films with different Mg compositions were carried out. Using theoretical simulation to the measured spectra, we obtained bandgap changes of the $Mg_xZn_{1-x}O$ films versus temperature and the possible physical mechanism for a new phenomenon observed in the low-temperature transmission measurements is discussed.

2. Experiments

The $Mg_xZn_{1-x}O$ thin films were grown on *c*-plane (0001) sapphire substrates at low temperature using reactive electron beam evaporation. High-purity ceramic targets of $(MgO)_x(ZnO)_{1-x}$ porcelain materials were prepared by sintering ZnO and MgO at the temperature of 1250 °C with different atomic ratios of Mg to Zn. All samples were grown at the substrate temperature of 250 °C with the oxygen background pressure of 2×10^{-4} Torr. During the growth, the working vapour pressure was kept constant at 3.5×10^{-4} Torr and the growth rate was about ∼25 nm min^{-1}. Further details of the growth procedure have been described in the references published previously [4, 6]. Compared with the growth temperature of 650–750 °C using pulsed laser deposition (PLD) [3] and 400 °C in the radio frequency magnetron sputtering method [7], the low-temperature growth technology used for $Mg_xZn_{1-x}O$ thin films has several advantages. Low growth temperature can minimize outgas of the components in the growth chamber, thus keeping the growth chamber clean. Particularly, when the $Mg_xZn_{1-x}O$ is grown on silicon, the low substrate temperature can prevent oxygen from diffusing into Si substrates because the $Mg_xZn_{1-x}O$ is grown in oxiding ambient. The thicknesses of the films were measured by an alpha-step profiler and surface roughness was measured by an atomic force microscope (AFM). PLA-SPECI inductively coupled plasma (ICP) was used to determine the Mg compositions in the ternary alloys. The x-ray diffraction (XRD) was measured by a Philips X'Pert x-ray diffraction to determine the crystalline structures. The temperature-dependent transmission measurements were performed by a Jobin-Yvon 460 monochromator with a variable-temperature (10–300 K) closed-cycle refrigerator system and a resolution of 5 Å.

3. Results and discussion

The $Mg_xZn_{1-x}O$ films grown on sapphire substrates are highly transparent and have mirror-like surface. The atomic force microscope (AFM) measurements showed that the roughness of the surface is smaller than 2 nm, indicating good surface quality. The ICP measurements of Mg

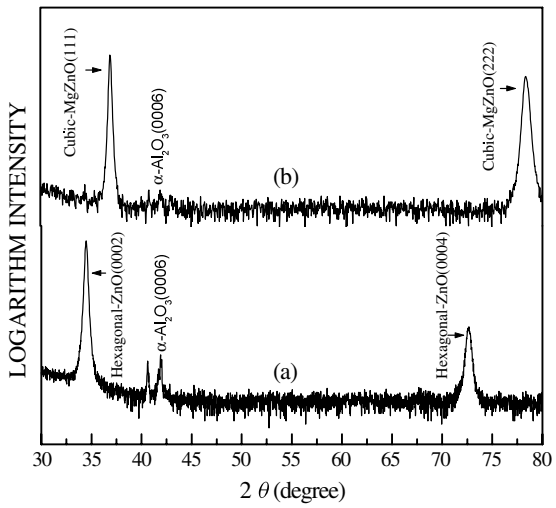

Figure 1. X-ray diffraction patterns: (a) hexagonal ZnO thin film grown on sapphire substrate; (b) cubic $Mg_{0.55}Zn_{0.45}O$ thin film grown on sapphire substrate.

concentration in the cubic $Mg_xZn_{1-x}O$ crystal films are consistent with the results obtained by ultraviolet transmission and simulation; for example, the ICP measurement of Mg composition of 54.2% is in good agreement with the data of 55% obtained by transmission measurement and simulation.

The XRD results for hexagonal ZnO and cubic $Mg_{0.55}Zn_{0.45}O$ films are shown in figures 1(a) and (b), respectively. Besides the twin substrate diffraction peaks at $2\theta = 40.64°$ and 41.90° shown in figure 1, the peaks at $2\theta = 34.54°$ and 72.72° are the diffraction of (0002) and (0004) planes of the hexagonal ZnO, respectively. The (111) and (222) diffraction peaks for the cubic $Mg_{0.55}Zn_{0.45}O$ film are at $2\theta = 36.93°$ and 78.33°, that are close to the calculations of diffraction peaks at $2\theta = 36.94°$ and 78.63° for cubic MgO(111) and (222) planes, respectively. No signatures of the hexagonal phase are observed in samples with Mg composition higher than 55%, which indicates that the $Mg_xZn_{1-x}O$ films ($x \geqslant 0.55$) possess only cubic-phase structure. The slightly smaller diffraction angles for cubic $Mg_{0.55}Zn_{0.45}O$ than MgO could be attributed to the Zn atoms substituting for Mg atoms partially in the cubic MgO lattice. Because the ionic radius of Zn^{2+} (0.83 Å) is bigger than Mg^{2+} (0.78 Å), the incorporation of Zn atoms into the cubic MgO lattice would enlarge the lattice constant of $Mg_{0.55}Zn_{0.45}O$ and the measured diffraction angles would be slightly smaller than those of MgO. The full width at half maximum (FWHM) of the (111) diffraction peak for the cubic $Mg_{0.55}Zn_{0.45}O$ is 0.22°, which is comparable to that of the (0002) diffraction peak for the hexagonal ZnO film, 0.23°. The broadening of the FWHM is attributed defects in the oxide films, such as dislocations and stacking faults.

Further XRD characterizations of the cubic $Mg_xZn_{1-x}O$ samples with different film thicknesses from 0.1 to 2.0 μm show that the phase transition from cubic to hexagonal crystal has not been observed when film thickness increases. However, different substrates have an effect on the orientation of the cubic $Mg_xZn_{1-x}O$ growth. The cubic $Mg_xZn_{1-x}O$ thin films deposited on Si substrate are (001) oriented [4], in contrast to the (111) orientation as grown on sapphire substrate [3].

Figure 2 exhibits the temperature-dependent transmittance spectra of the ZnO film. The experimental data are plotted in dotted curves and the theoretical fitting results are shown

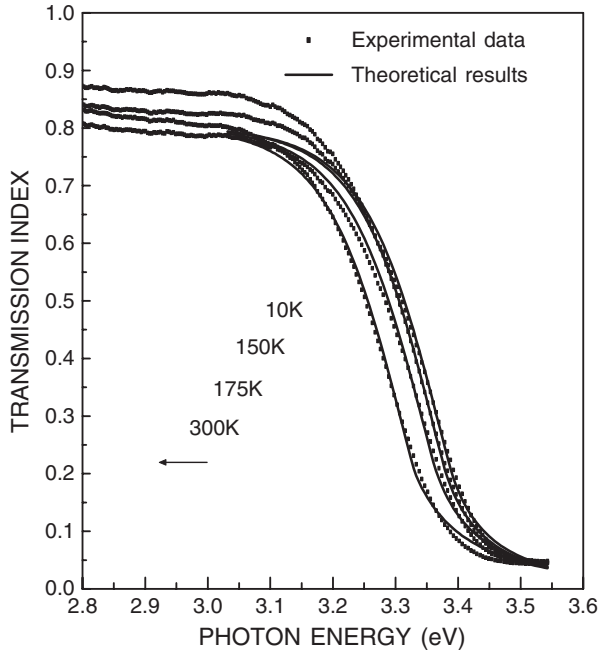

Figure 2. Transmittance spectra for the hexagonal ZnO film at the different temperatures. Dotted curves are experimental data and solid curves are theoretical fitting transmissions.

in solid curves. With increase of the measurement temperature, the absorption edge shifts to lower energies. However, as shown in figure 2 the quantity of shift is smaller than other wide-bandgap materials, such as GaN. The shift in the low-temperature region (10–150 K) is smaller than that in the high-temperature region (150–300 K). The small shift leads to an inaccuracy in determining the bandgap energy (E_g) by the normally used linear-extrapolated method. To determine the bandgap accurately, theoretical fitting to the measured transmittance spectra was used. The effects of optical absorption, multiple reflections and dispersion of the refractive index in the ZnO epitaxy on the transmission were included in the calculation. The dispersion of the refractive index can be expressed using the following formula:

$$n^2 = 1 + \frac{A_0\lambda^2}{\lambda^2 - \lambda_0^2}, \tag{1}$$

where A_0 and λ_0 are fitting parameters that are 2.60 and 211.4 (nm) for ZnO, respectively [8].

The optical absorption of ZnO thin films includes intrinsic square-root absorption and the Urbach exponential absorption [9]. The band tail in the low-energy region is due to the Urbach effect, which is very sensitive to the line shape of the spectra. Several mechanisms were responsible for the effect of the Urbach band tail in semiconductors, such as carrier–impurity interaction, carrier–phonon interaction, and structural disorder. Also indirect band transitions involved with phonons scattering in the direct bandgap material contribute to the Urbach band tail effect [10]. Here the impurity band tail and the electron–phonon interaction are the primary reasons to form the Urbach band tail because oxygen vacancies are prone to form in the hexagonal ZnO material. The Urbach band tail effect is included in the theoretical model as a fitting parameter that modifies the absorption coefficient on the lower-energy side ($h\nu < E_g$). Thus, the optical absorption coefficient of the ZnO film can be expressed as

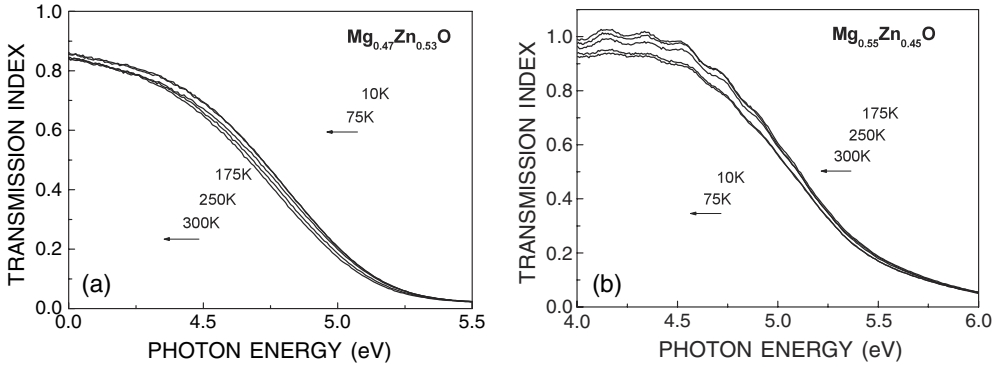

Figure 3. Temperature-dependent transmittance spectra of (a) the $Mg_{0.47}Zn_{0.53}O$ film and (b) the $Mg_{0.55}Zn_{0.45}O$ film, respectively.

follows [9]:

$$\alpha(h\nu) = \begin{cases} \alpha_0 \exp[(h\nu - E_e)/E_u] & (h\nu < E_g) \\ \alpha_d (h\nu - E'_g)^{1/2} & (h\nu \geqslant E_g). \end{cases} \tag{2}$$

Where E_e coincides with the energy of the lowest free exciton energy at 0 K, E'_g is the bandgap energy of the material without band tailing distortions and E_u is the Urbach band tail parameter. These material parameters, including α_0 and α_d, are linked through the continuity at the bandgap energy of E_g.

As shown in figure 2, the fitting transmittances (solid curves) are in reasonable agreement with the measured transmittance spectra (dot curves), particularly in the region of the absorption edge (3.2–3.4 eV). From the fitted results, we find that the absorption edge shifts only 60 meV throughout the whole temperature region from 10 to 300 K, in contrast to the shift of 140 meV for hexagonal, wide-bandgap GaN material [11]. The obtained temperature-dependent bandgap energy for ZnO can be expressed as $E_g(T) = 3.391 - 0.0003T^2/(T + 132.53)$ (eV). It corresponds to the general formulation of $E_g(T) = E_g(0) + \alpha T^2/(T + \beta)$ (eV) for semiconductor materials [10], with the negative temperature coefficient $\alpha = -0.0003$ eV K^{-1}. The E_g values of ZnO at 10 and 300 K are 3.39 and 3.33 eV, respectively, which is slightly different from the data listed in [11]. The reason for the small shift of absorption edge could be attributed to the fact that the measured optical absorption edge by transmittance spectra involved exciton transitions rather than band–band transition.

Figure 3 shows the transmittance spectra for the $Mg_xZn_{1-x}O$ films with Mg mole fractions $x = 0.47$ and 0.55. In comparison with ZnO film, the slope of the absorption edge for $Mg_xZn_{1-x}O$ film is smaller, but optical transmission in the low-energy region is higher ($\sim$90%) because of the wider bandgap of the $Mg_xZn_{1-x}O$ alloys. The modulation phenomenon appearing in the transmittance spectra in figure 3(b) is due to film interference. It can be seen in figure 3 that for $Mg_xZn_{1-x}O$ with $x = 0.47$, the absorption edge red shifts monotonically with increase of temperature. However, for the $Mg_xZn_{1-x}O$ samples with $x = 0.55$, the shift of absorption edge displays an abnormal phenomenon: as the temperature increases from 10 to 150 K, the absorption edge red shifts by a small amount. Then, as the temperature increases from 150 to 175 K, it abruptly shows a blue shift and reaches a peak at the temperature of 200 K, but with further increase of temperature from 200 to 300 K the absorption edge red shifts again. This abnormal phenomenon implies that Mg concentration in $Mg_xZn_{1-x}O$ is an important factor to influence the temperature-dependent optical absorption. Further transmittance measurements of other samples with different Mg compositions show that for

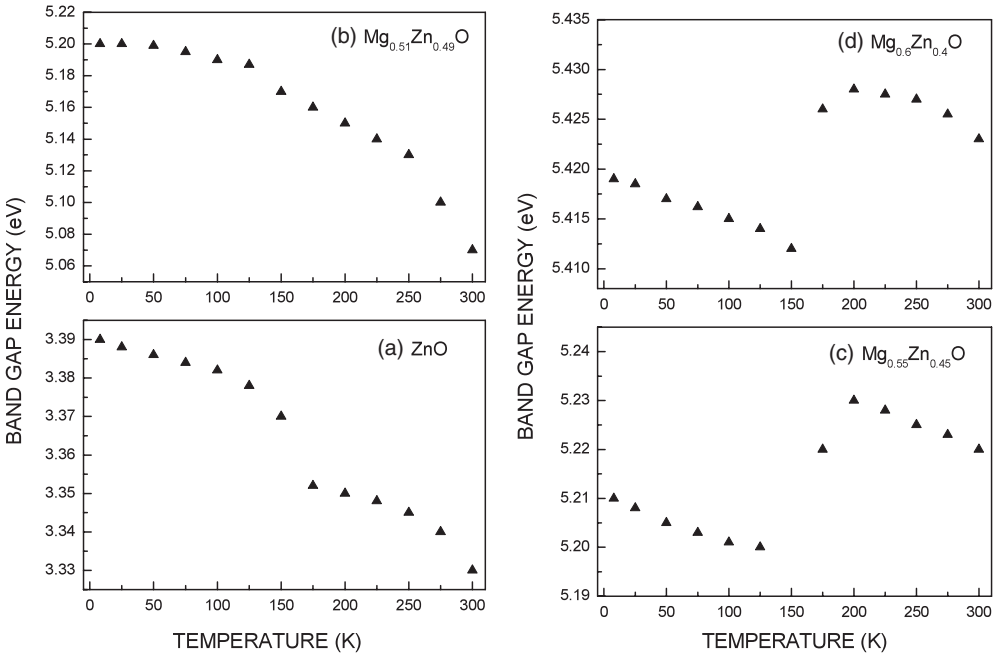

Figure 4. Temperature-dependent bandgap energies obtained by theoretical fitting: (a) the ZnO film, (b) the $Mg_{0.51}Zn_{0.49}O$ film, (c) the $Mg_{0.55}Zn_{0.45}O$ film and (d) the $Mg_{0.6}Zn_{0.4}O$ film, respectively.

$Mg_xZn_{1-x}O$ samples with $x \leqslant 0.51$ the absorption edge red shifts monotonically with increase of temperature, while for samples with $x \geqslant 0.55$ changes of absorption edge with temperature show the abnormal phenomenon.

Compared with the transmittance spectra of ZnO shown in figure 2, the absorption edges for $Mg_xZn_{1-x}O$ films shown in figure 3 are found to have smaller slopes. This phenomenon has been observed in other ternary compound semiconductor materials as well, which is attributed to the random distribution of Mg in the ternary $Mg_xZn_{1-x}O$ film alloys. Chen *et al* [12] have already studied the distribution of the Mg composition of x in the ternary $Mg_xZn_{1-x}O$ thin-film alloys. In the simulation of the absorption edge for the $Mg_xZn_{1-x}O$ film alloys, the effect of Mg distribution on optical absorption is also included.

The last factor to be considered in the simulation of optical absorption is the dispersion of the refractive index for $Mg_xZn_{1-x}O$ alloys. However, to date the refractive indices for $Mg_xZn_{1-x}O$ alloys with high Mg concentration ($x > 0.4$) are not available. Linear interpolation with refractive indices for ZnO and MgO is used and A_0, λ_0 parameters in equation (1) are deduced as functions of Mg concentration according to the results of [8]:

$$A_0 = 0.5086x^2 - 1.0954x + 2.6007 \tag{3}$$

$$\lambda_0 = -53.9073x^2 - 104.2304x + 210.5956 \text{ (nm)}. \tag{4}$$

Figure 4 shows the temperature-dependent bandgap energies of $Mg_{0.51}Zn_{0.49}O$, $Mg_{0.55}Zn_{0.45}O$ and $Mg_{0.6}Zn_{0.4}O$ films by simulation. For comparison, the result for ZnO is also given in figure 4(a). It is known that even if the Mg concentration (x) in the $Mg_xZn_{1-x}O$ film is as high as 0.49 the film crystalline structure is still hexagonal [5]. As shown in figure 4(b), the observed temperature characteristic of the bandgap for the $Mg_{0.51}Zn_{0.49}O$ film decreases with temperature, similar to the hexagonal ZnO and having a negative temperature coefficient.

This observation implies that even if the Mg concentration is up to 51%, the $Mg_xZn_{1-x}O$ film still has a stable hexagonal-phase crystal structure.

Interestingly, it is seen from figures 4(c) and (d) that as temperature increases from 10 to 150 K the bandgap (E_g) for the two cubic-phase samples shrinks by about 10 meV. Then the E_g value enlarges abruptly at the temperature of 150–175 K and reaches a maximum at about 200 K. Above 200 K E_g decreases monotonically. The total shift of the bandgap (temperature from 10 to 300 K) is only about 10 meV, that is much smaller than that for ZnO (60 meV). This temperature characteristic of the bandgap for the $Mg_xZn_{1-x}O$ film is also different from other wide-bandgap materials, such as aluminium nitride (AlN), for which a near linear shrinkage of E_g ($\sim$100 meV) was observed as temperature increased from 0 to 300 K [13]. We attribute this abnormality to the possible change of crystalline structure of the $Mg_xZn_{1-x}O$ ($x \geqslant 0.55$) films from cubic to hexagonal phase. Similarly, Choopun *et al* reported that the metastable cubic phase $Mg_xZn_{1-x}O$ ($x = 0.5$–1) could be obtained by controlling the growth temperature and a rapid annealing to the $Mg_xZn_{1-x}O$ films deposited at room temperature could cause the single cubic phase to be separated into both hexagonal and cubic phases [3]. The phase transition from cubic to hexagonal structure was also observed in metastable cubic GaN material [14].

A possible explanation for the phase transition observed in figures 4(c) and (d) is as follows. It is known that hexagonal oxygen vacancies are prone to form in MgZnO crystal [15]. An appreciable deviation from stoichiometry which results from the existence of the oxygen vacancies and the residual strain originating from the lattice mismatch between the $Mg_xZn_{1-x}O$ film and sapphire substrate lead to the existent of stacking faults at the grain boundary in the cubic $Mg_xZn_{1-x}O$ films [16, 17]. Because of the difference of thermal expansion coefficient between $Mg_xZn_{1-x}O$ and sapphire substrate, the strain in the cubic $Mg_xZn_{1-x}O$ increases when the measurement temperature decreases from 300 to 10 K. The compressive stress caused by the shrinkage of the crystal lattice is applied to the cubic $Mg_xZn_{1-x}O$ epitaxial layer. The compressive stress and the instability of the atoms around the stacking faults possibly change the cubic phase into more stable hexagonal phase and make the crystal orientation along the c-axis of hexagonal phase. Thus, for the $Mg_{0.55}Zn_{0.45}O$ and $Mg_{0.6}Zn_{0.4}O$ films shown in figures 4(c) and (d), the observed abnormality of the temperature-dependent absorption edge results from the phase transition from cubic phase to more stable hexagonal phase as measurement temperature decreases. Within the temperature range from 300 to 200 K, the bandgap variation represents cubic-phase characteristics, while from 150 to 10 K the bandgap change is similar to the hexagonal-phase one. The turning point for the phase transition is at about 150–175 K, similar to the phase transition point at about 150–200 K for the $K_{1-x}Li_xMnF_3$ single-crystal film [18]. The abnormality of the temperature-dependent bandgap variation at about 150–175 K can be attributed to the possible phase transition between cubic phase and hexagonal phase.

4. Conclusion

Both hexagonal $Mg_xZn_{1-x}O$ ($x \leqslant 0.51$) and cubic $Mg_xZn_{1-x}O$ ($x \geqslant 0.55$) films were grown on c-plane (0001) sapphire substrate at a temperature of 250 °C. X-ray diffraction measurements show that the cubic $Mg_xZn_{1-x}O$ films grow along the [111] direction while the hexagonal ZnO films grow along [0001]. The FWHM of the (111) diffraction peak for the cubic $Mg_xZn_{1-x}O$ (0.22°) is comparable to that of the (0002) diffraction peak for the hexagonal ZnO (0.23°). The measurements of temperature-dependent ultraviolet optical transmission and theoretical simulation of the optical absorption spectra showed that for the hexagonal $Mg_xZn_{1-x}O$ ($x \leqslant 0.51$) the optical absorption edge red shifts with temperature monotonically, similar to hexagonal ZnO. However, for the cubic $Mg_xZn_{1-x}O$ ($x \geqslant 0.55$), as

measurement temperature increases an optical absorption edge abnormality is observed at about 175 K. This abnormal phenomenon for the cubic $Mg_xZn_{1-x}O$ ($x \geqslant 0.55$) films is attributed to the possible phase transition from cubic to hexagonal structure when the measurement temperature decreases from 300 to 10 K. The underlying physical mechanism for the crystal phase transition is the interaction of stress with stacking faults in the cubic $Mg_xZn_{1-x}O$.

Acknowledgment

This work was supported by the Natural Science Foundation of China under grant Nos 10174064 and 10125416.

References

[1] Look D C 2001 *Mater. Sci. Eng.* B **80** 383
[2] Ohtomo A, Kawasaki M, Koida T, Masubuchi K, Koinuma H, Sakurai Y, Yoshida Y, Yasuda T and Segawa Y 1998 *Appl. Phys. Lett.* **72** 2466
[3] Choopun S, Vispute R D, Yang W, Sharma R P and Venkatesan T 2002 *Appl. Phys. Lett.* **80** 1529
[4] Qiu D J, Wu H Z, Chen N B and Xu T N 2003 *Chin. Phys. Lett.* **20** 582
[5] Park W I, Yi G C and Jang H M 2001 *Appl. Phys Lett.* **79** 2022
[6] Wu H Z, He K M, Qiu D J and Huang D M 2000 *J. Cryst. Growth* **217** 131
[7] Jeong S, Kim B and Lee B 2003 *Appl. Phys. Lett.* **82** 2625
[8] Teng C W and Muth J F 2000 *Appl. Phys. Lett.* **76** 979
[9] Shen W Z, Jiang L F, Yang H F and Meng F Y 2002 *Appl. Phys. Lett.* **80** 2063
[10] Shen X C (ed) 1992 *Optical Character of Semiconductors* (Beijing: Science Publishing Company)
[11] Kaldis E (ed) 1981 *Current Topics in Materials Science* vol 7 (Amsterdam: North-Holland) pp 143–482
[12] Chen J, Shen W Z, Chen N B, Qiu D J and Wu H Z 2003 *J. Phys.: Condens. Matter* **15** L475
[13] Tang X, Hossain F, Wongchotigul K and Spencer M G 1998 *Appl. Phys. Lett.* **72** 1501
[14] Okumura H, Ohta K, Feuillet G, Balakishnan K, Chichibu S, Hamaguchi H, Hacke P and Yoshida S 1997 *J. Cryst. Growth* **178** 113
[15] Vanheusden K, Warren W L, Seager C H, Tallant D R, Voigt J A and Gnade B E 1996 *J. Appl. Phys.* **79** 7983
[16] Cho H K, Lee J Y, Kim K S and Yang G M 2000 *J. Cryst. Growth* **220** 197
[17] Yang-Bitterlich W, Bitterlich H, Zahn G and Kramer U 2002 *J. Alloys Compounds* **347** 131
[18] Waskowska A and Ratuszna A 1998 *J. Solid State Chem.* **137** 71